Journal of Renewable and Sustainable Energy, Volume 16, April 2024, Article number 024702
DOI: 10.1063/5.0190664

Experimental investigation of wave induced flapping foil for marine propulsion: heave and pitch stiffness effect

Junxian Wang,[1] Jingru Xing,[1] M. Salman Siddiqui,[2] Adriana Stawiarska,[1] and Liang Yang[1]
[1)]*Division of Energy and Sustainability, School of Water, Energy and Environment (SWEE), Cranfield University, Bedford MK43 0AL, United Kingdom*
[2)]*Department of Mechanical Engineering and Technology Management, Norwegian University of Life Sciences, Drøbakveien 31, Ås, 1432, Ås, Norway*

(*Electronic mail: liang.yang@cranfield.ac.uk)

(Dated: 30 April 2024)

The submerged hydrofoil has the capability to harness wave energy and convert it into thrust to work with the ship's power system. The current series of experiments investigated the interaction of a passive submerged hydrofoil with regular waves through a comparison of the generated horizontal forces. Springs provide the restoring force for the hydrofoil's heave/pitch motion, corresponding to heave spring and pitch spring. Maintaining a constant heave spring stiffness (490 N/m), subsequent statistical analysis summarized the force trends at different pitch stiffness (16 N/m to 300 N/m) and suggested an optimal pitch spring stiffness in regular waves. A pulse-shaped force signal was observed and explained as a result of low pitch stiffness. Experiments with different spring setups revealed that the heave spring contributes to the harmonic force generated by the fully passive foil. Additionally, by varying wave conditions with limited wave amplitudes and frequencies, tests reproduced the variation of force signals over time and assessed their dependence on wave parameters.

I. INTRODUCTION

When subjected to wave excitation, a floating structure can exhibit a response with six degrees of freedom (DoF), including heave and pitch. One popular application of this principle is in wave energy converters (WECs) equipped with suitable power take-off (PTO) systems, which can harvest energy from waves and convert it into electricity[1]. Inspired by the movements of birds and fish, the flapping motion of a foil-shaped structure, specifically heaving and pitching, can generate thrust and power[2,3]. Consequently, another wave energy application is the use of a submerged foil that undergoes flapping motion in waves, effectively harnessing wave energy and directly converting it into propulsion[4–6]. This application of wave energy holds enormous potential for powering vessels and has the capability to replace traditional propulsion system. Additionally, research has shown that attaching a foil to the bottom of a ship can stabilise its motion and reduce resistance[7]. An example of an experienced hydrofoil application is the wave glider[8–10]. Furthermore, the study of active-pitch control foils[11–15] generating thrust for ships in waves has gained significant attention in recent years.

The investigation of a flapping foil typically involves prescribing its constraints or motion, resulting in three configurations: fully active[16], semi-passive[17,18], or fully passive. Passive foils often incorporate the installation of springs, such as single spring-dominated DoF (i.e., semi-passive), or dual spring-dominated DoFs (heave and pitch, i.e., fully passive). The inclusion of springs has been found to enhance power generation and achieve excellent power conversion efficiency[19,20], while also affecting the hydrofoil's dynamic characteristics[21]. Feng et al.[22] conducted numerical studies on a semi-passive foil using nonlinear pitch springs and observed a multi-frequency phenomenon during the propulsion process. Wang et al.[23] performed a two-dimensional numerical simulation on a fully passive foil and observed harmonic inertia force signals. Additionally, investigations have revealed the significant impact of spring stiffness on the loads and dynamic behaviour of the foil, including the flapping amplitude and the advance speed[19,24–27]. It is worth noting that the previous investigations mentioned above primarily focused on spring stiffness in semi-passive foils. Therefore, further studies are needed to examine the impact of pitch spring stiffness and heave spring stiffness on fully passive foils.

In terms of experimental studies conducted in a single-phase flow, extensive model tests have been carried out on foils with various constraints and prescribed motions[19,20,28–31]. When considering the interaction with real waves, semi-passive or fixed foils have been attached underneath ships to assess their effectiveness in improving stability, power, and reducing ship resistance[32–37]. As for investigation about fully passive foils in waves, when the hydrofoil is equipped with power take-off (PTO) system, the relative heave motion between the foil and the surface floater can be converted into electrical power, forming a hybrid propulsion system[38]. Isshiki and Murakami[39,40] carried out a series of experiments on a submerged fully passive foil in response to regular waves, with a focus on the impact of heave stiffness and wavelength. It is obvious that limited previous experimental studies on the interaction between fully passive foils and waves indicate a significant research gap. Furthermore, a systematic study comparing dual spring-dominated DoFs (heave and pitch), single spring-dominated DoF (heave or pitch), and the fully fixed mode is necessary to explore the effect of the spring system.

As a result, the current study involved a series of experiments on a fully passive hydrofoil in regular waves, with variations in pitch spring stiffness, spring-dominated DoF, and wave parameters. The time history of the horizontal force was recorded and subjected to statistical analysis. The results reveal averaged force trends in relation to pitch stiffness and suggested an optimal pitch stiffness for excellent thrust gen-

eration. Furthermore, the results observed and explained the pulse-shaped force signal caused by small pitch stiffness, as well as the higher harmonic response in the force-time series due to the heave spring. These findings provide a comprehensive understanding of the impact of the spring system on the interaction between waves and fully passive foils, thereby guiding the application of fully passive foils on ships.

II. METHODOLOGY

A. Experimental setup

Experiments for the present study were performed in a wave tank located at Cranfield University[41], featuring 30 m long, 1.5 m wide, and 1.5 m of designed water depth. A piston-type wave generator near one end of the tank enabled the generation of regular and irregular waves, up to the wave height limit of 0.28 m. To minimise wave reflection, a wave absorber and an absorption beach are placed at both ends of the tank. The test section is positioned around 8.4 m away from the wave paddle. The design and construction of the experimental rig were inspired by Isshiki and Murakami[39,40]. The 3D hydrofoil model used in the study is of the NACA0024 type, fabricated through 3D printing. The hydrofoil has a chord length (c) of 0.2 m and a span length (b) of 0.1 m (refer to Figure 1). Two pivot points on the chord line are located 25 mm (P1) behind the leading edge (A) and 20 mm (P2) in front of the trailing edge (B).

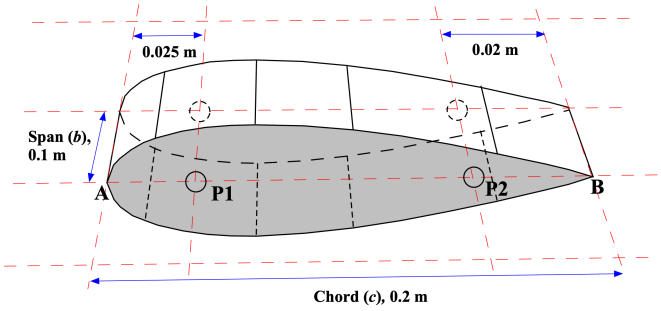

FIG. 1. Schematic sketch of NACA0024 hydrofoil.

The experimental setup, as depicted in Figure 2, comprises a top carriage, a middle connection (rod R1 and R2), the spring system, and the hydrofoil model. Notably, the 3D effect exists due to no end-plates being fixed to the hydrofoil. A compression heave spring (hS) is installed within the front rod (R1) to control the hydrofoil's heaving motion, while extension pitch springs (pS) is attached to the rear rod (R2) to adjust the hydrofoil's pitching motion. The hydrofoil's surge motion was disabled due to the top carriage remaining fixed throughout this study. The selected heave spring keeps a constant stiffness (k_{hS}), while pitch springs feature various stiffness (k_{pS}) with two different arrangements. For detailed schematic sketches and descriptions of the experimental setup, please refer to Wang et al.[42]. The Hooke's Law equation suggests that

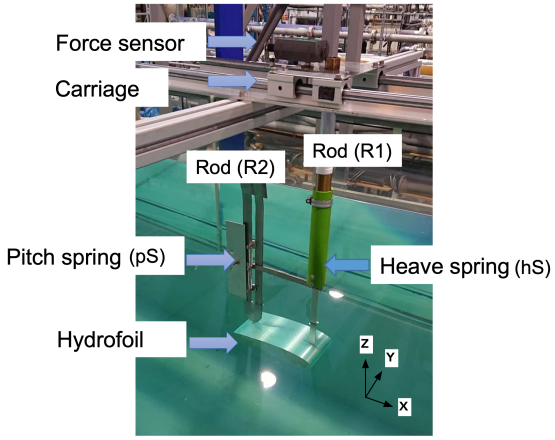

FIG. 2. Schematic sketch of experimental setup.

connecting two identical extension springs axially can double the length change and thus halve the effective stiffness. Therefore, one configuration involves placing one pitch spring on each side, as shown in Figure 2, while the other arrangement includes two identical pitch springs on each side. Prior to conducting experiments, we measured the natural frequency of the experimental setup by tapping the top carriage and the front rod, respectively. The recognised frequency exceeded 10 Hz, which is significantly higher than the measured force signal (Figure 3b), indicating the negligible impact of the front rod (R1).

B. Experimental conditions and data analysis

A multi-functional "Go Direct®" load cell was installed on the top carriage to collect the horizontal force. This load cell is capable of measuring forces within the range of $\pm$50 N, detecting force increments down to 0.002 N. The sampling frequency for force collection is 50 Hz to guarantee a smooth signal and accurate signal peaks. For this study, we investigated the impact of pitch stiffness (k_{pS}) via collecting and analyse the generated horizontal force. This involved testing a total of 12 different effective stiffness values, ranging from 16 N/m to 300 N/m, to encompass significant flapping amplitude and angle changes. The hydrofoil was submerged at a depth of around 0.1 m, driven by foil's significant pitch motion and the higher wave energy near the free surface. The hydrofoil starts in its neutral position due to the equilibrium between the pre-load difference of the pitch spring on both sides and the buoyancy, with the chord line parallel to the water surface. We adopted specific wave parameters, including wave amplitudes (A_W) of 0.04 m, 0.05 m, and 0.06 m, and wave frequencies (f_W) of 0.75 Hz, 0.85 Hz, and 1 Hz. These wave parameters were chosen to verify the reliability of the recorded force data and its correlation to wave conditions. To explore the effect of the spring setup, the experiment reduced the hydrofoil's degrees of freedom from 2 to 1 by disabling either the heaving or pitching motion, resulting in "pitch spring

only" or "heave spring only" foils. Additionally, the experiment further reduced the degrees of freedom to 0, resulting in a fully fixed foil. As a result, the experimental cases are summarised in Table I and II. Cases 1 to 12 illustrate the impact of pitch stiffness, while the comparison among cases 9 and 16 to 19 highlights the effects of wave amplitude and frequency. Cases 13 to 15 are designed to investigate the influence of the number of spring-dominated DoF. To ensure experiment validity, each case was repeated either 10 or 5 times, as indicated in the "repeat" column of Table I and II.

To process the data, we employed force spectral analysis using the Discrete Fourier Transform (DFT) method. Additionally, we applied phase-averaging techniques to accurately assess load variation throughout a single cycle. The collected horizontal force signal from this horizontally fixed foil exhibits a periodic oscillation near zero value. Our previous studies[42] about the running hydrofoil revealed its advance displacement, as well as the backward shift at each cycle. The positive part of horizontal force signal and the negative part can be inferred to affect the forward and backward displacement of the running foil, respectively. As a result, apart from the collected horizontal force (F_X), two additional force-related terms were discussed: the positive force (F_P) and the negative force (F_N). Corresponding time-averaged values can be calculated:

$$\overline{F_X} = \frac{1}{t}\int_0^t F_X(t_0)\mathrm{d}t_0, \tag{1}$$

$$\overline{F_P} = \frac{1}{t}\int_0^t (F_X > 0)(t_0)\mathrm{d}t_0, \tag{2}$$

$$\overline{F_N} = \frac{1}{t}\int_0^t (F_X < 0)(t_0)\mathrm{d}t_0, \tag{3}$$

where t stands for time length of a given force signal and F_X is the instantaneous horizontal force. As experiment for each case was repeated 10 or 5 times, the standard error of the mean (SEM) is calculated as follows:

$$\sigma_{\bar{i}} = \frac{\sigma_i}{\sqrt{n}}, \tag{4}$$

where σ_i is standard deviation of a given length signal and n is signal number obtained from repeat testing. And thus force-related terms after correction can be expressed as:

$$\overline{F_X'} = \frac{\sum_{j=1}^{n}\overline{F_X}(j)}{n} \pm \frac{\sigma_X}{\sqrt{n}}, \tag{5}$$

$$\overline{F_P'} = \frac{\sum_{j=1}^{n}\overline{F_P}(j)}{n} \pm \frac{\sigma_P}{\sqrt{n}}, \tag{6}$$

$$\overline{F_N'} = \frac{\sum_{j=1}^{n}\overline{F_N}(j)}{n} \pm \frac{\sigma_N}{\sqrt{n}}, \tag{7}$$

where the first item on the right-hand refers to the mean value after repeat testing.

Case	DoF	k_{pS} (N/m)	k_{hS} (N/m)	f_W (Hz)	A_W (m)	Repeat
1	2	16	490	0.75	0.05	10
2	2	24	490	0.75	0.05	10
3	2	30	490	0.75	0.05	10
4	2	48	490	0.75	0.05	10
5	2	60	490	0.75	0.05	10
6	2	70	490	0.75	0.05	10
7	2	90	490	0.75	0.05	10
8	2	110	490	0.75	0.05	10
9	2	130	490	0.75	0.05	10
10	2	160	490	0.75	0.05	10
11	2	230	490	0.75	0.05	10
12	2	300	490	0.75	0.05	10

TABLE I. Summary of testing cases (Case 1 to 12).

Case	DoF	k_{pS} (N/m)	k_{hS} (N/m)	f_W (Hz)	A_W (m)	Repeat
13	1	Max[a]	490	0.75	0.05	10
14	1	130	Max	0.75	0.05	10
15	0	Max	Max	0.75	0.05	10
16	2	130	490	0.75	0.06	5
17	2	130	490	0.75	0.04	5
18	2	130	490	0.85	0.05	5
19	2	130	490	1	0.05	5

[a] Max: DoF of this direction is disabled.

TABLE II. Summary of testing cases (Case 13 to 19).

III. RESULTS AND DISCUSSION

Based on the arrangements shown in Table I and II, this section primarily presents a comparison of forces obtained from experimental tests, considering the influence of pitch stiffness (16 N/m to 300 N/m), the number of spring-loaded degrees of freedom (2, 1, 0), wave amplitudes (0.04m, 0.05m, 0.06m), and wave frequencies (0.75 Hz, 0.85 Hz, 1 Hz). Statistical analyses on the horizontal force (F_X), as well as its positive (F_P) and negative (F_N)components, reveal the influence of the heave/pitch spring on force variation. Specially, The force changing against pitch spring stiffness (k_{pS}) suggested an optimal stiffness range. The emergence of the pulse-shaped force is attributed to smaller pitch stiffness. Comparison on different spring setups proved that the heave stiffness is related to the harmonic force response.

Firstly, a preliminary study is presented involving a representative single test with a pitch stiffness of k_{pS} = 70 N/m, as shown in Figure 3. The time series plot of force variation in Figure 3a clearly shows seven stable cycles at the wave frequency, indicating that this low-frequency fluctuation is induced by wave excitation. Additionally, the higher-frequency fluctuation is observed within each cycle. The corresponding spectrum in Figure 3b reveals the primary frequency of 0.75 Hz, which corresponds to the wave frequency, and the presence of the forth, fifth harmonic representing the additional fluctuation. This phenomenon of higher harmonics has been observed in previous research involving wave interactions with semi-passive foils[22] and single-phase flow in-

teractions with fully passive foils[23]. However, what distinguishes our findings is the significant amplitude of the additional fluctuation in the force signal. Specifically, the high-frequency portion oscillates dramatically within one cycle, as highlighted using red dashed squares and blue markers in Figure 3a. Detailed explanation about this force signal with pitch stiffness of k_{pS} = 30, 130 N/m can be found in Wang et al.[42].

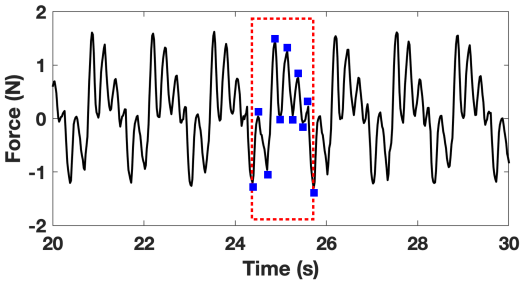

(a)

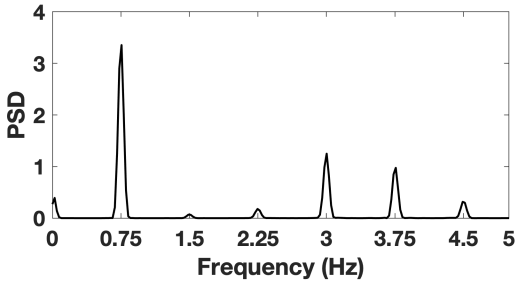

(b)

FIG. 3. Force analysis about a single test from Case 6 (k_{pS} = 70 N/m, k_{hS} = 490 N/m, 2DoFs, A_W 0.05 m, f_W 0.75 Hz): (a) Time series of force; (b) Spectra of force.

A. Pitch stiffness

Using equations (5), (6), and (7), forces after correction (i.e., $\overline{F'_P}$, $\overline{F'_N}$, $\overline{F'_X}$) were processed from all tests within the pitch stiffness range of 16 N/m to 300 N/m, and corresponding results are presented in Figure 4. In the figure, solid squares represent the mean forces, and the length of the vertical lines indicates the magnitude of the error. Notably, the forces tend to stabilise at lower levels as pitch stiffness increases towards pitch DoF being disabled (i.e., k_{pS} = Max). For example, $\overline{F'_N}$ approximately -0.8 N at $k_{pS} \geq$ 300 N/m, $\overline{F'_P}$ around 0.5 N for $k_{pS} \geq$ 110 N/m, and $\overline{F'_X}$ approximately 0.1 N for $k_{pS} \geq$ 230 N/m. Forces are higher at the lower pitch stiffness range of 16 N/m to 90 N/m. Specifically, $\overline{F'_P}$, $\overline{F'_N}$ exhibit optimal stiffness characteristics, and $\overline{F'_X}$ fluctuates around 0.15 N. During the transitional region, $\overline{F'_N}$ gently decreases from k_{pS} = 90 N/m to 230 N/m, followed by a significant drop from 230 N/m to 300 N/m. $\overline{F'_X}$ displays a gentle decreasing trend, while $\overline{F'_P}$ sharply decreases from k_{pS} = 90 N/m to 110 N/m. In summary, as the pitch stiffness increases till "Max", all forces decreases and tends to stabilize. $\overline{F'_P}$ and $\overline{F'_N}$ are outstanding and high at lower pitch stiffness, indicating an optimal stiffness range, Meanwhile, the $\overline{F'_X}$ is fluctuated at its high value.

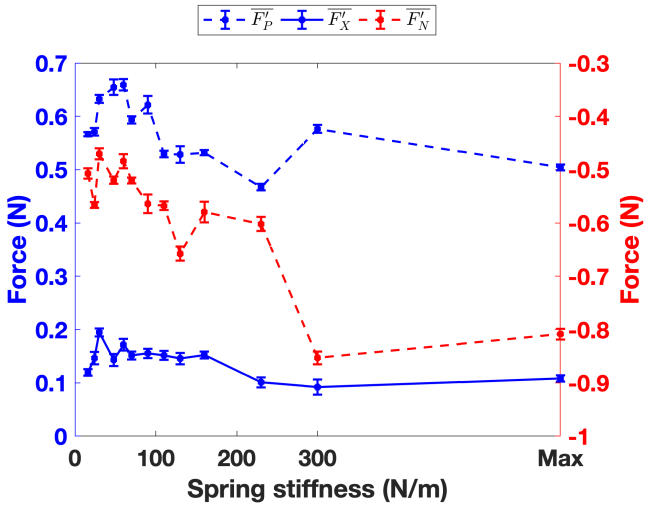

FIG. 4. Statistic analysis of pitch stiffness (Case 1 to 13).

The mean phase-averaged forces from repeated tests at different pitch stiffness values are shown in Figure 5, 6. These force profiles resemble the pattern seen in Figure 3a. A total of 10 peaks, marked with blue squares, are displayed in Figure 5f. Across all peaks, the significant local maximum and local minimum are selected and referred to as T1 and D1 respectively. At a pitch stiffness of k_{pS} = 16 N/m (Figure 5a), peak T1 stands out significantly, measuring 1.28 N (0.82π) compared to the following three local maxima, which are 0.72 N (1.21π), 0.14 N (1.58π), and 0.06 N (1.79π), respectively. This creates a pulse-shaped force variation. As stiffness increases, the dominance of peak T1 gradually diminishes, becoming comparable to the following local maxima after $k_{pS} \geq$ 110 N/m. Our previous related studies[42] documented and discussed the flapping angle at pitch stiffness values of k_{pS} = 30 N/m and 130 N/m. It was observed that the lower stiffness value (30 N/m) resulted in a larger flapping angle, consistent with trends from previous research[19,24–26]. These findings suggest that pitch stiffness influences the underwater pose and flapping angle of the foil, with lower stiffness values leading to larger flapping angles. Considering the similar trend in the significance of the pulse shape, it can be associated with the flapping angle. Specifically, lower pitch stiffness results in a larger flapping angle, contributing to the pulse-shaped force signal. The force summary in terms of peak T1 and D1 within an averaged cycle, varying with pitch stiffness, is described in Figure 7. As stiffness increases, the absolute force of T1 decreases, while that of D1 increases, until reaching a stable state at k_{pS} = Max.

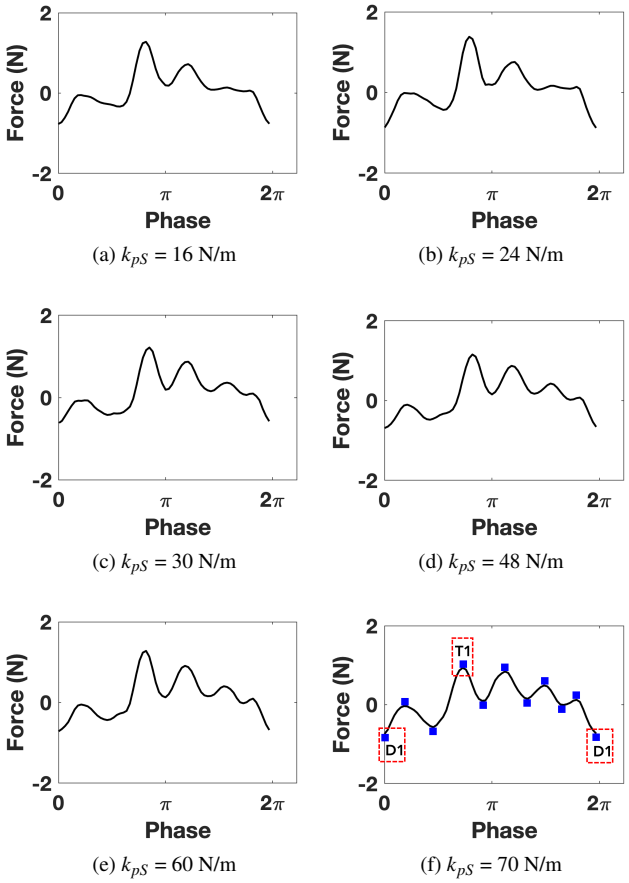

(a) k_{pS} = 16 N/m (b) k_{pS} = 24 N/m (c) k_{pS} = 30 N/m (d) k_{pS} = 48 N/m (e) k_{pS} = 60 N/m (f) k_{pS} = 70 N/m

FIG. 5. Summary of phase average (Case 1 to 6), (a) - (f) describe results at the pitch stiffness range of 16 N/m to 70 N/m.

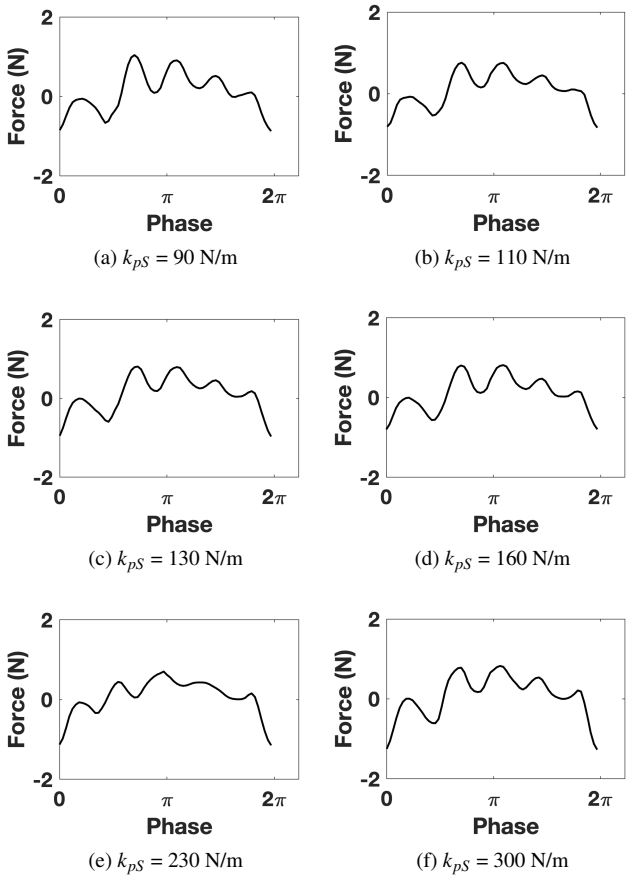

(a) k_{pS} = 90 N/m (b) k_{pS} = 110 N/m (c) k_{pS} = 130 N/m (d) k_{pS} = 160 N/m (e) k_{pS} = 230 N/m (f) k_{pS} = 300 N/m

FIG. 6. Summary of phase average (Case 7 to 12), (a) - (f) describe results at the pitch stiffness range of 90 N/m to 300 N/m.

B. Spring-dominated DoF

Similar harmonic force observed in Figure 3 has been previously observed in research on passive foils[22,23]. However, the amplitude of the high-frequency fluctuation in Figure 3a is significantly larger than what has been reported in the aforementioned research. This difference may be attributed to the presence of the pitch/heave spring system. To investigate this further, this subsection conducts experiments with different configurations, including single spring-dominated DoF (e.g., pitch spring only or heave spring only), zero DoF (fully fixed), and compares the results to those obtained with two spring-dominated DoFs. It's important to note that a foil with one spring-dominated DoF can be considered a semi-passive foil.

Spectral analysis of single test force signals for different pitch/heave arrangements is presented in Figure 8a. These arrangements include pitch (pS) and heave (hS) spring (k_{pS} = 130 N/m, k_{hS} = 490 N/m), pitch spring only (k_{pS} = 130 N/m, k_{hS} = Max), heave spring only (k_{pS} = Max, k_{hS} = 490 N/m), and fully fixed (k_{pS} = Max, k_{hS} = Max). Figure 8a shows six harmonic frequencies: 1st order (0.75 Hz), 2nd order (1.5 Hz), 3rd order (2.25 Hz), 4th order (3 Hz), 5th order (3.75 Hz), and 6th order (4.5 Hz). All four cases share the same primary frequency, the 1st order (0.75 Hz), which corresponds to

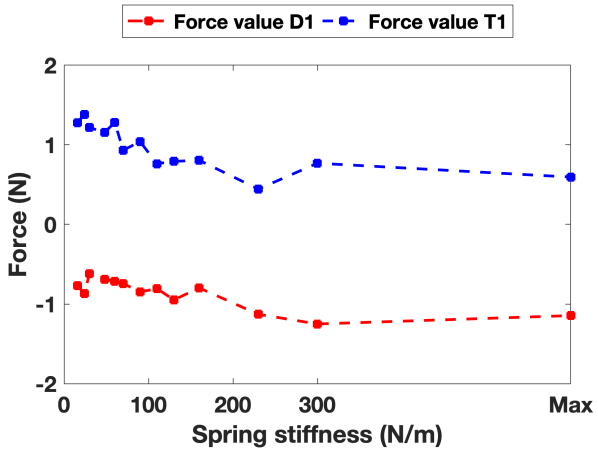

FIG. 7. Thrust peak (T1) and drag peak (D1) variation against pitch stiffness (Case 1 to 13).

the wave frequency. However, they differ in higher frequencies. In the fully fixed case, apart from the primary frequency, higher frequency peaks are not apparent, indicating that the regular wave excitation causes a single-frequency force sig-

nal. In the pitch-only case, the 2nd frequency is distinct compared to the fully fixed case, confirming previous research on semi-passive foil[22]. However, when the heave spring is installed, the spectral results for cases with and without pitch spring successfully detect the 2nd, 3rd, 4th and 5th frequencies. Additionally, the 5th order frequency (3.75 Hz) stands out. Correspondingly, the mean phase-averaging force curves for these four pitch/heave arrangements are shown in Figure 8b. In the comparison of different heave DoF arrangements (k_{hS} = 490 N/m and Max), the force variation is found to fluctuate with a high amplitude when the heave spring is activated at k_{hS} = 490 N/m. As for the pitch spring, the corresponding comparison suggests that it does not give rise to significant impact on the signal shape.

Consequently, the results in terms of modifying the spring-dominated DoF in this subsection confirm the harmonic phenomenon observed by previous research[22] when only activating the pitch degree of freedom, and furthermore provide pioneering evidence that the heave spring induces and dominates the outstanding higher-order frequencies and large high-frequency fluctuations. For this experimental study, all repeated cases for two spring-dominated DoFs (i.e., the coexistence of pitch and heave springs) recorded the harmonic force response with outstanding higher-order frequencies. However, it should be noted that some tests show varying numbers of outstanding higher-order frequencies, for instance the 4th and 5th orders in Figure 3b and the 5th order in Figure 8a. Furthermore, some different tests for the same k_{pS} and k_{hS} values differ in the number of outstanding higher-order frequencies, which may be attributed to the high sensitivity of the pitch and heave spring system.

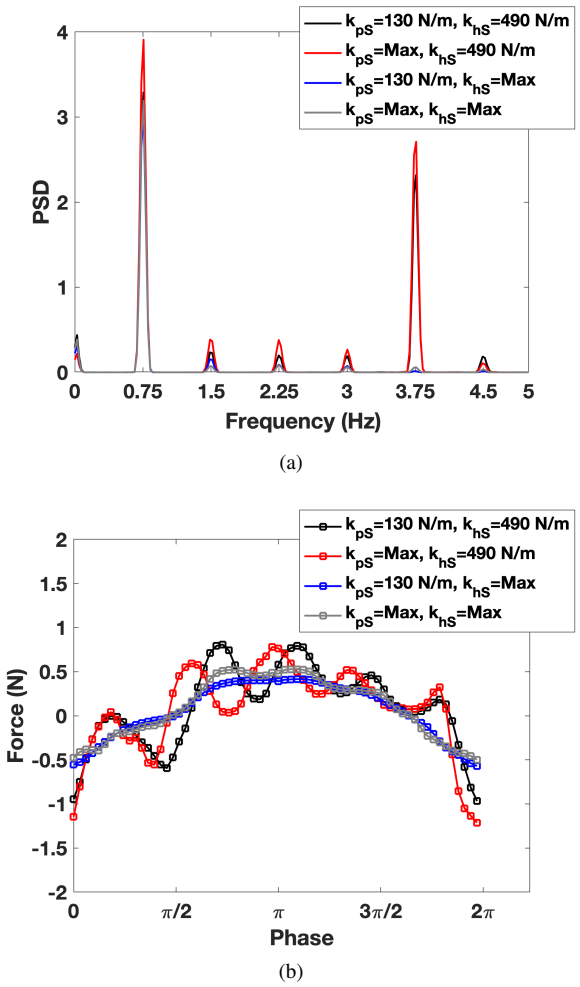

(a)

(b)

FIG. 8. Impact of number of spring-dominated DoF (Case 9, 13, 14, 15): (a) spectral analysis, (b) force variation.

C. Wave amplitude and frequency effect

This subsection aims to briefly verifying thrust performance at different regular waves and exploring the effect of wave conditions. It discusses various regular wave parameters, including wave amplitude (A_W = 0.04 m, 0.05 m, 0.06 m) and wave frequency (f_W = 0.75 Hz, 0.85 Hz, and 1 Hz), on a fully spring-loaded hydrofoil with pitch/heave stiffness of 130 N/m and 490 N/m. The corrected horizontal force ($\overline{F'_X}$), as well as its positive ($\overline{F'_P}$), negative ($\overline{F'_N}$), are presented in Figure 9a and Figure 9b. It is observed that $\overline{F'_P}$ and $\overline{F'_X}$ are dependent on changes in the tested wave amplitude range. Specifically, $\overline{F'_P}$ increases by 29% and 61% as the wave amplitude changes from 0.04 m to 0.05 m and 0.06 m, respectively, and $\overline{F'_X}$ increases by 57% and 162%. The absolute value of $\overline{F'_N}$ also increases from 0.52 N to 0.66 N as the wave amplitude increases from 0.04 m to 0.05 m. Considering the impact of wave frequency in Figure 9b, $\overline{F'_P}$ is found to increase within wave frequency range of 0.75 Hz to 1 Hz,, corresponding to force values of 0.53 N, 0.68 N, and 0.83 N, respectively.

IV. CONCLUSION

The present study investigates the variation of horizontal loads on a fully passive hydrofoil with spring-loaded heave and pitch in response to regular waves. The experimental setup focuses on examining the impact of spring stiffness (k_{hS} = 490 N/m, k_{pS} = 16 N/m to Max), spring-dominated DoFs, as well as wave parameters (A_W = 0.04 m, 0.05 m, 0.06 m, f_W = 0.75 Hz, 0.85 Hz, 1 Hz). Three force-related terms are considered: the horizontal force (F_X), and its positive component (F_P), negative component (F_N). Statistical analysis was employed to post-process force data including time and phase-averaging, as well as the mean value plus SEM. This study reveals interesting findings, which are summarised as follows:

- The variation of the pitch stiffness from k_{pS} = 16 N/m to Max exhibits leads to a decrease in horizontal force, its positive component and its negative component, eventually maintaining at a stable level. At lower pitch stiffness values, $\overline{F'_P}$ and $\overline{F'_N}$ suggested an optimal spring stiffness range for the outstanding force performance.

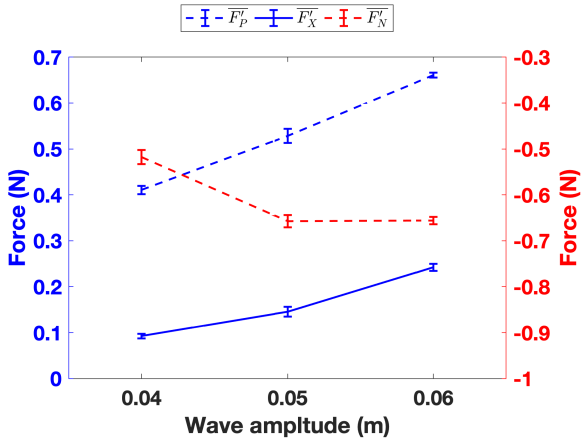

(a)

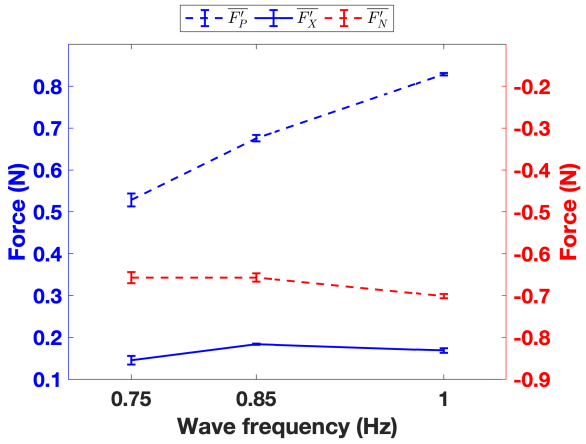

(b)

FIG. 9. Variation of $\overline{F'_P}$, $\overline{F'_X}$, $\overline{F'_N}$ at diverse wave conditions. (a): A_W = 0.04 m, 0.05 m, 0.06 m, f_W = 0.75 Hz; (b): f_W = 0.75 Hz, 0.85 Hz, 1 Hz, A_W = 0.05 m.

- Due to the harmonic force response, phase-averaging forces for different pitch stiffness display several peaks within the phase range of 0 to 2π, including one significant local maximum (T1), one local minimum (D1). At small pitch stiffness, peak T1 highlights the pulse-shaped signal possibly owing to hydrofoil's large flapping angle. This pulse shape gradually diminishes in significance with the increasing pitch stiffness.

- Investigation on spring-dominated DoF confirms the contribution of pitch spring on the observed harmonic phenomenon. Furthermore, the heave spring was found to directly contribute to the outstanding higher-order harmonic frequencies and higher harmonic force fluctuations with significant amplitudes.

- The positive component (F_P) of the total force shows a good correlation with changes within the tested wave amplitude range and wave frequency range.

V. LIMITATIONS AND FURTHER RECOMMENDATIONS

While our study has provided valuable insight into the impact of spring stiffness on fully passive hydrofoil interacting with regular waves, it is essential to acknowledge certain limitations that may affect the applicability of our results. The hydrofoil's scaled-down chord length being slightly larger, along with the 3D effect resulting from the model's low aspect ratio, may affect the assessment of full-scale marine propulsion systems. Due to the limited experimental equipment, non-dimensional force analysis and additional synchronized measurements are needed, including wave profiles, foil dynamics (heave and pitch), and flow fields near the model. Comparing results with different types of hydrofoil models could enhance the credibility of our findings. Lastly, a limited range of wave conditions were tested in this study, which may not sufficiently and effectively summarise its impact. Building on the findings of this study, we will further investigate the interaction of passive hydrofoils with waves, exploring various factors such as hydrofoil type, pivot location, the hydrofoil's forward speed and a wide range of wave parameters.

ACKNOWLEDGMENTS

L. Yang acknowledgement the support from the UK - Saudi Challenge Fund 'Feasibility study of hybrid propulsion for unmanned surface vehicle for environmental monitoring' and TRIG2022 grant from Department for Transport (DfT): 'G-TRANSPORT: Greening Transportation of Cargo Ships via Hybrid Wave Propulsion'.

DATA AVAILABILITY

The data that support the findings of this study are available from the corresponding author, L. Yang, upon request.

DECLARATION OF COMPETING INTEREST

The authors declare that they have no known competing financial interests or personal relationships that could have appeared to influence the work reported in this paper.

[1]J. H. Todalshaug, G. S. Ásgeirsson, E. Hjálmarsson, J. Maillet, P. Möller, P. Pires, M. Guérinel, and M. Lopes, "Tank testing of an inherently phase-controlled wave energy converter," International Journal of Marine Energy **15**, 68–84 (2016).
[2]R. Knoller, "Die gesetzedes luftwiderstandes," Flug-und Motortechnik (Wien) **3**, 1–7 (1909).
[3]A. Betz, "Ein beitrag zur erklaerung segelfluges," Z Flugtech Motorluftschiffahrt **3**, 269–272 (1912).
[4]T. Y. T. Wu, "Extraction of flow energy by a wing oscillating in waves," Journal of ship research **16**, 66–78 (1972).
[5]H. Isshiki, "A theory of wave devouring propulsion (1st report) thrust generation by a linear wells turbine," Journal of the society of naval architects of Japan **1982**, 54–64 (1982).
[6]J. Xing and L. Yang, "Wave devouring propulsion: An overview of flapping foil propulsion technology," Renewable and Sustainable Energy Reviews **184**, 113589 (2023).

[7]X. Wu, X. T. Zhang, X. L. Tian, X. Li, and W. Y. Lu, "A review on fluid dynamics of flapping foils," Ocean Engineering **195**, 106712 (2020).

[8]Z. Qi, M. Jiang, L. Jia, B. Zou, and J. Zhai, "The effect of mass ratio and damping coefficient on the propulsion performance of the semi-active flapping foil of the wave glider," Journal of Marine Science and Engineering **8**, 303 (2020).

[9]W.-Q. Wang, W. Li, Y. Yan, and J. Zhang, "Parametric study on the propulsion and energy harvesting performance of a pitching foil hanging under a wave glider," Renewable Energy **184**, 830–844 (2022).

[10]Z. Qi, B. Zou, H. Lu, J. Shi, G. Li, Y. Qin, and J. Zhai, "Numerical investigation of the semi-active flapping foil of the wave glider," Journal of Marine Science and Engineering **8**, 13 (2019).

[11]E. Filippas and K. Belibassakis, "A nonlinear time-domain bem for the performance of 3d flapping-wing thrusters in directional waves," Ocean Engineering **245**, 110157 (2022).

[12]K. Belibassakis and E. Filippas, "Ship propulsion in waves by actively controlled flapping foils," Applied Ocean Research **52**, 1–11 (2015).

[13]G. K. Politis and V. T. Tsarsitalidis, "Flapping wing propulsor design: An approach based on systematic 3d-bem simulations," Ocean engineering **84**, 98–123 (2014).

[14]E. Filippas and K. Belibassakis, "Hydrodynamic analysis of flapping-foil thrusters operating beneath the free surface and in waves," Engineering Analysis with Boundary Elements **41**, 47–59 (2014).

[15]S.-W. Huang, T.-L. Wu, Y.-T. Hsu, J.-H. Guo, J.-F. Tsai, and F.-C. Chiu, "Effective energy-saving device of eco-ship by using wave propulsion," in *2016 Techno-Ocean (Techno-Ocean)* (IEEE, 2016) pp. 566–570.

[16]L. W. A. De Silva and H. Yamaguchi, "Numerical study on active wave devouring propulsion," Journal of marine science and technology **17**, 261–275 (2012).

[17]J. Wu, Y. L. Qiu, C. Shu, and N. Zhao, "Pitching-motion-activated flapping foil near solid walls for power extraction: A numerical investigation," Physics of Fluids **26**, 083601 (2014).

[18]M. Boudreau, K. Gunther, and G. Dumas, "Free-pitching flapping-foil turbines with imposed sinusoidal heave," Journal of Fluids and Structures **90**, 110–138 (2019).

[19]E. Bøckmann and S. Steen, "Experiments with actively pitch-controlled and spring-loaded oscillating foils," Applied Ocean Research **48**, 227–235 (2014).

[20]M. Boudreau, G. Dumas, M. Rahimpour, and P. Oshkai, "Experimental investigation of the energy extraction by a fully-passive flapping-foil hydrokinetic turbine prototype," Journal of Fluids and Structures **82**, 446–472 (2018).

[21]J. R. Xing, D. Stagonas, P. Hart, C. C. Zhang, J. H. Yang, and L. Yang, "Wave induced thrust on a submerged hydrofoil: pitch stiffness effects," arXiv preprint arXiv:2209.05551 (2022), 10.48550/arXiv.2209.05551.

[22]Z. X. Feng, Z. Y. Chang, C. Deng, L. Zhao, J. Chen, J. K. Zhang, and Z. Q. Zheng, "Effects of nonlinearity of restoring springs on propulsion performance of wave glider," Nonlinear Dynamics **108**, 2007–2022 (2022).

[23]Z. Wang, L. Du, J. S. Zhao, and X. F. Sun, "Structural response and energy extraction of a fully passive flapping foil," Journal of Fluids and Structures **72**, 96–113 (2017).

[24]Z. Y. Chang, Z. X. Feng, C. Deng, L. Zhao, J. K. Zhang, Z. Q. Zheng, and Z. J. Yu, "Analysis of propulsion performance of wave-propelled mechanism based on fluid-rigid body coupled model," Proceedings of the Institution of Mechanical Engineers, Part M: Journal of Engineering for the Maritime Environment **236**, 713–725 (2022).

[25]H. Q. Sang, G. Liu, X. J. Sun, C. Li, L. Wang, and L. W. Wang, "Hydrodynamic performance analysis of flapping hydrofoil for single-body architecture wave glider," Ocean Engineering **261**, 112118 (2022).

[26]N. Thaweewat, S. Phoemsapthawee, and V. Juntasaro, "Semi-active flapping foil for marine propulsion," Ocean Engineering **147**, 556–564 (2018).

[27]W. Chen, Y. Zhang, and F. Gao, "Experimental and numerical studies on the torsion stiffness effect of a semi-active flapping hydrofoil propulsion," Ocean Engineering **265**, 112578 (2022).

[28]L. Duarte, N. Dellinger, G. Dellinger, A. Ghenaim, and A. Terfous, "Experimental investigation of the dynamic behaviour of a fully passive flapping foil hydrokinetic turbine," Journal of Fluids and Structures **88**, 1–12 (2019).

[29]Y. Zhang, Y. Feng, W. Chen, and F. Gao, "Effect of pivot location on the semi-active flapping hydrofoil propulsion for wave glider from wave energy extraction," Energy **255**, 124491 (2022).

[30]A. W. Mackowski and C. H. K. Williamson, "Effect of pivot location and passive heave on propulsion from a pitching airfoil," Physical Review Fluids **2**, 013101 (2017).

[31]D. A. Read, F. S. Hover, and M. S. Triantafyllou, "Forces on oscillating foils for propulsion and maneuvering," Journal of Fluids and Structures **17**, 163–183 (2003).

[32]E. Bøckmann and S. Steen, "The effect of a fixed foil on ship propulsion and motions," in *Proceedings of the Third International Symposium on Marine Propulsors smp*, Vol. 13 (2013) pp. 553–561.

[33]J. A. Bowker and N. C. Townsend, "Evaluation of bow foils on ship delivered power in waves using model tests," Applied Ocean Research **123**, 103148 (2022).

[34]J. A. Bowker, M. Tan, and N. C. Townsend, "Forward speed prediction of a free-running wave-propelled boat," IEEE Journal of Oceanic Engineering **46**, 402–413 (2020).

[35]E. Bøckmann and S. Steen, "Model test and simulation of a ship with wavefoils," Applied Ocean Research **57**, 8–18 (2016).

[36]S. Naito and H. Isshiki, "Effect of bow wings on ship propulsion and motions," Applied Mechanics Reviews **58**, 253–268 (2005).

[37]C. Chan, J. Wang, L. Yang, and J. Zang, "Wave-assisted propulsion: An experimental study on traveling ships," Physics of Fluids **36** (2024), 10.1063/5.0190630.

[38]J. Bowker, N. Townsend, M. Tan, and R. Shenoi, "Experimental analysis of submerged flapping foils; implications for autonomous surface vehicles (asvs)," in *OCEANS 2016 MTS/IEEE Monterey* (IEEE, 2016) pp. 1–10.

[39]H. Isshiki and M. Murakami, "A theory of wave devouring propulsion (3rd report) an experimental verification of thrust generation by a passive-type hydrofoil propulsor," Journal of the Society of Naval Architects of Japan **1983**, 118–128 (1983).

[40]H. Isshiki and M. Murakami, "A theory of wave devouring propulsion (4th report) a comparison between theory and experiment in case of a passive-type hydrofoil propulsor," Journal of the society of naval architects of Japan **1984**, 102–114 (1984).

[41]N. Mailh, *Experimental investigation of lift and drag on the NACA 4412 near the water surface*, Ph.D. thesis, Cranfield University (2017).

[42]J. Wang, S. Santhosh, O. Colomés, M. Capaldo, and L. Yang, "Experimental study of dynamic response of passive flapping hydrofoil in regular wave," Physics of Fluids **35** (2023), 10.1063/5.0157890.